Project THEMIS
Technical Report No. 13

PENETRATIVE CONVECTIVE INSTABILITIES IN PARALLEL FLOWS

by

René A. Kahawita

and

Robert N. Meroney

Prepared under

Office of Naval Research

Contract No. N00014-68-A-0493-0001

Project No. NR 062-414/6-6-68(Code 438)

U. S. Department of Defense

Washington, D. C.

Fluid Dynamics and Diffusion Laboratory
College of Engineering
Colorado State University
Fort Collins, Colorado

May, 1972

CER71-72-RK-RNM-24

ABSTRACT

An analysis has been performed of penetrative convective instabilities arising from the combined action of thermal and centrifugal buoyancy forces. The theory allows for the fact that in the atmosphere, convection arising in an unstable layer may penetrate into a neighboring stable region. The objective has been to examine the effect of various mean temperature and velocity profiles on the critical limit and convective penetration of the disturbances. The linearized perturbation equations have been solved employing an approximate technique. The results obtained indicate that nonlinear profiles are more unstable and penetrative than linear ones. The close analogy between streamline curvature and thermal stratification effects has been demonstrated. It is found that for parallel layers of fluid along curved heated walls, a unique stability curve for neutral disturbances may be obtained if the quantity plotted along the abscissa is $Ra + \kappa N_G^2$ where Ra is the Rayleigh Number, N_G is the Goertler Number and κ a constant which expresses the relative importance of the mean temperature and velocity profiles.

TABLE OF CONTENTS

LIST OF FIGURES

LIST OF SYMBOLS

Symbol	Definition
$\tilde{u}$	Horizontal velocity perturbation
$\tilde{v}$	Vertical velocity perturbation
$\tilde{w}$	Lateral velocity perturbation
$\tilde{p}$	Pressure perturbation
$\tilde{T}$	Temperature perturbation
U	Mean flow (undisturbed) horizontal velocity
T	Mean temperature
k	Curvature
Pr	Prandtl Number
N_G	Goertler Number
Ra	Rayleigh Number
x,y,z	Streamwise, vertical and lateral directions, respectively
R_δ	Reynold's Number $(= \frac{U_\infty \delta}{\nu})$
c	Penetration coefficient
d	Total depth of penetration
g	Gravitational acceleration
t	Time
f	Dimensionless velocity profile
T_*	Dimensionless temperature $(= \frac{T - T_w}{T_\infty - T_w})$
ΔT	Temperature difference across unstable layer
β	Volumetric expansion coefficient
ν	Kinematic viscosity
χ	Stability parameter
Φ	Dimensionless wavenumber

LIST OF SYMBOLS - (Continued)

Symbol	Definition
δ	Characteristic thickness of boundary layer
ξ	Transformed vertical coordinate
α	Wavenumber

Subscript	
p	y dependent part of perturbations
w	Conditions at wall $(y = 0)$
∞	Conditions at edge of unstable layer $(y = \delta)$

PENETRATIVE CONVECTIVE INSTABILITIES IN PARALLEL FLOWS

I. INTRODUCTION

This discourse considers penetrative convective instabilities resulting from the combined action of thermal and centrifugal buoyancy forces. These instabilities are assumed to take the form of steady three dimensional vortices oriented in the streamwise direction and are similar to the disturbances observed in the flow between rotating concentric cylinders. The latter instability manifests itself in the form of regularly spaced toroidal vortices stacked around the inner cylinder. This phenomenon was first examined by Taylor (1) who formulated the motion in mathematical terms, analyzed its stability and verified the analysis in quite conclusive fashion. If the inner cylinder is sufficiently far removed that the flowfield reduces to that of a boundary layer along a curved wall, the instabilities induce a secondary flow of parallel streamwise oriented vortices. Goertler (2) and later Smith (3) investigated the vortex mode of motion along a plate with concave curvature and indicated the presence of a system of parallel counter rotating vortices aligned in the mean flow direction. Furthermore, their analyses clearly indicated that only flows with concave curvature were susceptible to this type of instability. Experimental verification was subsequently obtained by Goertler (2), Liepmann (4) and Tani (5). The parameter governing the stability of the flow is the Goertler Number $R_\delta \sqrt{k\delta}$ where R_δ is the Reynolds Number based on the boundary layer thickness, δ , and k is the curvature of the wall.

The analogy between flows with concave curvature and buoyancy due to unstable stratification was pointed out by Goertler (6) and more recently by Yih (7) and by Bradshaw (8). Terada (9) and Sparrow et al. (10), have observed the vortex mode of motion in the flows of liquids down inclined heated plates.

The occurrence of a closely analogous phenomenon in the atmosphere is fairly well documented. The large-scale cloud streets frequently observed in satellite photographs are now accepted as direct evidence of the presence of longitudinal vortex instabilities in the earth's atmosphere. The clouds are formed as a result of the convective action of the rolls in lifting moist air to its condensation level. Further direct evidence is supplied by the experience of glider pilots (11), who have made use of these 'invisible highways' in the air to soar over large distances. Kuo (12) analyzed the stability of plane Couette flow with a suitable gradient of potential temperature so as to model the atmospheric boundary layer. However, his boundary conditions required the physically unrealistic situation of a rigid upper bounding surface.

The present study allows for the fact, that in the atmosphere, convection arising in an unstable layer may penetrate into a neighboring stable region. This in fact, was implied in a paper by Kuettner (11) who observed that cloud streets frequently had well defined tops indicating the presence of an elevated inversion. An additional consideration is that when there is a mean shear, the role of penetrative convection in vertical transfer of heat, moisture, and momentum may be important, as indicated in a recent paper by Estoque (13). The penetrative action of the instabilities into the stable region may be due to two causes, viz., a) the nonvanishing of the vertical velocity components of the disturbances at the interface causing inertial penetration or b) momentum being transferred into the upper layer by viscous interaction of the perturbations with the adjoining stable fluid. The outer system of vortices observed in Taylor's experiment was due to this second type of penetration.

Inertial penetration has been studied extensively (see, for example, Stix (14), and Whitehead and Chen (15)), while penetration by viscous entrainment has been studied recently by Rintel (16). The analysis described herein, assumes that the penetration is of the second type and follows closely the work of Rintel. In this approximation, the instabilities generated in a layer of fluid of thickness δ , penetrate to a total height d into neighboring stable fluid. A quantity $c = \frac{d}{\delta}$ called the penetration coefficient provides an estimate of the degree of penetration.

Solutions have been obtained for a variety of flows along heated curved walls with stable* fluid overhead. In most cases, the *raison d'etre* has been to model atmospheric type† instabilities and to demonstrate more clearly the analogy existing between flows with concave curvature and unstable stratification. Consequently, the Tollmein-Schlichting wave-type disturbances pertinent to transtion are not accounted for in this analysis. However, for heated or curved flow-fields the Squire theorem does not necessarily hold (17); hence three dimensional disturbances may be the more unstable mode. Furthermore, these stationary convective motions have been observed to persist in turbulent fluid by Tani (5) where the problem of transition does not arise. The specific cases of the parallel flows whose stability

*In this context 'stable' refers to stability with respect to velocity gradient, i.e., where Rayleigh's inviscid stability criterion is satisfied as well as the conventional interpretation of stable temperature stratification.

†It is realized of course, that the atmospheric situation is complex, with anistropic turbulent diffusivities of heat and momentum. Nevertheless, some qualitative results may be inferred.

are examined herein are:

a) Heated flat plate boundary layer

b) Parallel flow with free surface along curved heated walls

c) Boundary layer type flow with wall curvature and heating bounded above by fluid with differing stable gradients of temperature and velocity

d) Stationary layer of fluid with strongly non-linear temperature distribution bounded by mildly stable fluid

e) Stationary layer of fluid with parabolic mean temperature profile posed as a problem in penetrative convection

Details of the cases examined will be discussed later.

II. Theoretical Development

Consider an unstably stratified parallel flow over a curved surface. The unstable layer is considered to be bounded above by fluid of neutral or arbitrarily specified stability. It is assumed that the disturbances generated in the lower layer of thickness δ penetrate to a height d. The penetration coefficient is then defined as $c = \frac{d}{\delta}$. The parameter c thus provides a measure of the extent of penetration. In this respect it is closely allied to the "effective depth" defined by Kuo (12).

We start with the Navier-Stokes equations of motion and the energy equation, expressed in a curvilinear coordinate system (Fig. (1)). Using the Boussinesq approximation, one can derive the following equations for the perturbations $\tilde{p}$, $\tilde{T}$, $\tilde{u}_i$ of pressure, temperature and the three components of velocity, respectively.

$$\frac{\partial \tilde{u}}{\partial t} + \tilde{v}\frac{\partial U}{\partial y} + k\tilde{v}U + \tilde{w}\frac{\partial U}{\partial z} = \nu\left\{\frac{\partial^2 \tilde{u}}{\partial y^2} + \frac{\partial^2 \tilde{u}}{\partial z^2} + k\frac{\partial \tilde{u}}{\partial y}\right\}$$

$$\frac{\partial \tilde{v}}{\partial t} - 2k\tilde{u}U = g\beta\tilde{T} - \frac{1}{\rho}\frac{\partial \tilde{p}}{\partial y} + \nu\left\{\frac{\partial^2 \tilde{v}}{\partial y^2} + \frac{\partial^2 \tilde{v}}{\partial z^2} + k\frac{\partial \tilde{v}}{\partial y}\right\} \tag{1}$$

$$\frac{\partial \tilde{w}}{\partial t} = -\frac{1}{\rho}\frac{\partial \tilde{p}}{\partial z} + \nu\left\{\frac{\partial^2 \tilde{w}}{\partial y^2} + \frac{\partial^2 \tilde{w}}{\partial z^2} + k\frac{\partial \tilde{w}}{\partial y}\right\}$$

$$\frac{\partial \tilde{v}}{\partial y} + \frac{\partial \tilde{w}}{\partial z} + k\tilde{v} = 0 \tag{2}$$

$$\frac{\partial \tilde{T}}{\partial t} + \tilde{v}\frac{\partial T}{\partial y} + \tilde{w}\frac{\partial T}{\partial z} = \frac{\nu}{P_r}\left\{\frac{\partial^2 \tilde{T}}{\partial y^2} + \frac{\partial^2 \tilde{T}}{\partial z^2} + k\frac{\partial \tilde{T}}{\partial y}\right\} \tag{3}$$

where k denotes the curvature, ν, the kinematic viscosity, β, the volume expansion coefficient and g the gravitational acceleration. One can analyze an arbitrary disturbance into a set of normal modes

$$\tilde{u} = u_p(y) \ \text{Cos}\ \alpha z \ e^{\beta_1 t}$$

$$\tilde{v} = v_p(y) \ \text{Cos}\ \alpha z \ e^{\beta_1 t}$$

$$\tilde{w} = w_p(y) \ \text{Sin}\ \alpha z \ e^{\beta_1 t}$$

$$\tilde{T} = T_p(y) \ \text{Cos}\ \alpha z \ e^{\beta_1 t}$$

$$\tilde{p} = p_p(y) \ \text{Cos}\ \alpha z \ e^{\beta_1 t}$$

and since we consider only neutral disturbances we substitute the above disturbances into equations (1) to (3) with $\beta_1 = 0$. The justification for this step lies in the validity of the principle of the "exchange of stabilities" for such flows (15,18). This results in the following system of differential equations:

$$v_p\left(\frac{\partial U}{\partial y} + kU\right) = -\nu\{u_p'' + ku_p' - \alpha^2 u_p\} \tag{4}$$

$$2kUu_p = g\beta T_p - \frac{p_p'}{\rho} + \nu\{v_p'' + kv_p' - \alpha^2 v_p\} \tag{5}$$

$$0 = \alpha \frac{p_p}{\rho} + \nu\{w_p'' + kw_p' - \alpha^2 w_p\} \tag{6}$$

$$0 = v_p' + kv_p + \alpha w_p \tag{7}$$

$$v_p \frac{\partial T}{\partial y} = \frac{\nu}{P_r} \{T_p'' + kT_p' - \alpha^2 T_p\} \tag{8}$$

α is of course the horizontal wavenumber of the perturbations.

For solution of these equations, the 'rigid-free' boundary conditions (Chandrasekhar (18)) are assumed. That is, the plane $y = 0$ is taken to be a rigid surface with $y = \delta$ being a free surface.

The boundary conditions are then

$$v_p = (D^2 - \alpha^2)^2 v_p = 0 \quad \text{for} \quad y = 0 \quad \text{and} \quad \delta$$

$$v_p' = 0 \quad \text{at} \quad y = 0 \quad \text{and} \quad v_p'' = 0 \quad \text{at} \quad y = \delta$$

By eliminating p_p and w_p and discarding higher order curvature terms, equations (4) to (8) may be reduced to

$$(D^2 - \alpha^2)^2 v_p = \frac{\alpha^2}{\nu} (g\beta T_p - 2kUu_p) \tag{9}$$

$$(D^2 - \alpha^2) u_p = \frac{-v_p}{\nu} (\frac{\partial U}{\partial y} + kU) \tag{10}$$

$$(D^2 - \alpha^2) T_p = \frac{Pr}{\nu} \frac{\partial T}{\partial y} v_p \tag{11}$$

Here $D \equiv \frac{d}{dy}$ and U and T refer to the undisturbed mean velocity and temperature respectively.

Defining dimensionless quantities $\phi = \alpha\delta$, $Ⓗ' = \frac{g\beta\delta^2}{\nu}$, $\gamma' = \frac{2kU_\infty\delta^2}{\nu}$, $R_\delta = \frac{U_\infty\delta}{\nu}$, $f = \frac{U}{U_\infty}$, $f' = \frac{\partial f}{\partial y}$, $T_*' = \frac{\partial T}{\partial y} \frac{1}{\Delta T}$ with y made dimensionless with respect to δ and ΔT the temperature difference across the fluid layer, equations (9), (10), and (11) become

$$(D^2 - \phi^2)^2 v_p = \phi^2 (Ⓗ' T_p - fu_p\gamma') \tag{9a}$$

$$(D^2 - \phi^2) u_p = - (v_p R_\delta f' + v_p R_\delta fk\delta) \tag{10a}$$

$$(D^2 - \phi^2) T_p = \delta \frac{Pr}{\nu} \Delta T \, T_*' v_p \tag{11a}$$

As stated earlier, the penetration coefficient c is defined as the ratio of the penetrated height d to the thickness δ of the unstable layer. We therefore define a new dimensionless coordinate

$\xi = \frac{y}{c}$ and the modified parameters $Ⓗ = c^2 Ⓗ'$, $\Phi = c\phi$, $\gamma = c^2\gamma'$ and a modified Reynolds Number $R_{c\delta} = cR_\delta$. Eliminating the second term on the right hand side of equation (10a) since the product $k\delta$ is always small, one obtains with the above dimensionless parameters the final form of the differential equations for the perturbations viz.,

$$(D^2 - \Phi^2)^2 v_p = \Phi^2(Ⓗ T_p - f(c\xi)u_p\delta) \tag{12}$$

$$(D^2 - \Phi^2) u_p = -v_p R_{c\delta} f'(c\xi) \tag{13}$$

$$(D^2 - \Phi^2) T_p = v_p Pr \frac{c\delta}{\nu} \Delta T \; T'(c\xi) \tag{14}$$

where $D \equiv \frac{d}{d\xi}$. The revised boundary conditions are

$$T_p = u_p = 0 \quad \text{for} \quad \xi = 0 \text{ and } 1$$

$$v_p = Dv_p = 0 \quad \text{for} \quad \xi = 0$$

$$v_p = D^2 v_p = 0 \quad \text{for} \quad \xi = 1$$

Equations (12) to (14) are solved approximately using a technique devised by Chandrasekhar (18). The parallel and normal to the wall components of the perturbation velocity are expanded in a series of functions satisfying the boundary conditions for a rigid wall at $\xi = 0$ and a free surface boundary at $\xi = 1$.

$$\begin{aligned} u_p &= \sum_{n=1}^{\infty} B_n x_n \\ v_p &= \sum_{n=1}^{\infty} A_n z_n \end{aligned} \tag{15}$$

The temperature perturbation, since it satisfies similar boundary conditions as u_p is written as

$$T_p = \sum_{n=1}^{\infty} C_n x_n \tag{15}$$

where we choose

$$\lambda_n x_n = \mathrm{Sin}\; n\pi\xi$$

$$\lambda_n^2 z_n = \lambda_n x_n + \frac{2n\pi}{\mathrm{Sinh}\; 2\Phi - 2\Phi}\{\mathrm{Sinh}\Phi\xi - \xi\mathrm{Sinh}\Phi\mathrm{Cosh}(\Phi\xi-\Phi)\}$$

$$\lambda_n^2 = n^2\pi^2 + \Phi^2$$

It may be readily verified that the functions chosen satisfy the boundary conditions and also that

$$(D^2 - \Phi^2)\; x_n = -\lambda_n x_n$$

$$(D^2 - \Phi^2)\; z_n = \lambda_n z_n$$

When these expressions are substituted into the differential equations and the coefficients B_n and C_n are eliminated, the following eigenvalue system is obtained for A_n .

$$A_n = c^3\Phi^2\{8N_G^2 \sum_{m=1}^{\infty} \frac{X'_{nm}}{\lambda_m} \sum_{\ell=1}^{\infty} \frac{A_\ell Y'_{\ell n}}{\lambda_\ell} + 2Ra\,\frac{1}{\lambda_n} \sum_{m=1}^{\infty} \frac{A_m}{\lambda_m} Y^o_{mn}\}$$

where $N_G = R_\delta\sqrt{k\delta}$ is the Goertler Number and $Ra = \frac{g\beta\delta^3\Delta T}{\nu K}$ is the Rayleigh Number with

$$X'_{nm} = \lambda_n\lambda_m \int_o^1 f x_m x_n d\xi$$

$$Y'_{\ell n} = \lambda_\ell\lambda_n \int_o^1 f' z_\ell x_n d\xi$$

$$Y^o_{mn} = \lambda_m\lambda_n \int_o^1 T' z_m x_n d\xi$$

The standard method of evaluating the Fourier coefficient has been used to arrive at the previous equation. It may now be rewritten as

$$A_n = c^3\Phi^2 \sum_{\ell=1}^{\infty} A_\ell \{8N_G^2 P_{\ell n} + 2RaQ_{\ell n}\} = c^3\Phi^2 \sum_{\ell=1}^{\infty} A_\ell R_{\ell n} \tag{16}$$

Here $Q_{\ell n} = \dfrac{Y^o_{\ell n}}{\lambda_\ell \lambda_n}$, $P_{\ell n} = \displaystyle\sum_{m=1}^{\infty} \frac{X'_{nm} Y'_{\ell m}}{\lambda_\ell \lambda_m}$

In matrix notation we have the familiar eigenvalue problem

$$[A] = \Phi^2 c^3 [R][A]$$

The equation of neutral stability is then

$$|\delta_{nm} - c^3\Phi^2 R_{nm}| = 0$$

To simplify numerical evaluation of equation (16), it is rewritten in the form

$$A_n = c^3\Phi^2 N_G^2 \sum_{\ell=1}^{\infty} A_\ell \{8P_{\ell n} + 2R_n Q_{\ell n}\} \tag{17}$$

where R_N is defined as $\dfrac{Ra}{N_G^2}$. It therefore expresses the relative importance of buoyancy forces to centrifugal inertial forces with viscous damping as an overall effect. Equation (17) was solved for various values of the R_N number.

III. Outline of Solution Procedure

Numerical evaluation of the eigenvalue problem was performed on a CDC 6400 computer. The method consisted in minimizing the Goertler or Rayleigh Number as a function of the wavenumber Φ and penetration coefficient c. The method is well described by Rintel (16). A complete neutral stability curve may be generated by varying Φ keeping c at its critical value. The results thus obtained are scaled with the critical c value. A more accurate representation would be obtained if c is minimized at each point on the stability curve. This, however, ceases to be economical in terms of computer time. For cases of combined heating with wall curvature, equation (17) was used with R_n being treated as a parameter. For purposes of numerical evaluation, the infinite series expansion in equation (15) was truncated to thirty terms and the matrices were limited to fifth order. For the cases where penetration was into neutrally stable fluid, the order of the matrices used was increased to nine. A check, performed by increasing the truncation order of both the series and the matrices, revealed that this provided sufficient accuracy.

The mean flow profiles for the cases examined are listed below.

(a) The heated flat plate boundary layer

$$f(y) = 2y - 2y^3 + y^4 \qquad 0 \leq \xi \leq \frac{1}{c}$$

matched at $\xi = \frac{1}{c}$ with

$$f(y) = \chi(2y - 2y^3 + y^4) + 1 - \chi \qquad \frac{1}{c} \leq \xi \leq 1$$

where $y = c\xi$ and χ is a parameter used to represent the stability of the outer "freestream" gradient. χ was set equal to 10^{-8} in this case, to represent a neutrally stable freestream. The Prandtl Number was taken as unity. Critical conditions were evaluated with two types of mean thermal profile, the first being identical to the Pohlhausen profile above and the second, a linear one:

$$T_*(y) = y \qquad o \leq \xi \leq \frac{1}{c}$$

$$T_*(y) = -\chi y \qquad \frac{1}{c} \leq \xi \leq 1$$

with $\chi = 10^{-8}$. Here $T_* = \frac{T - T_w}{T_\infty - T_w}$ where T_∞ = temperature at edge of unstable layer, T_w = wall temperature.

(b) Parallel flow with free surface along curved heated wall

$$f(y) = y(2 - y)$$

$$T_*(y) = y$$

were assumed for the mean velocity and temperature profiles respectively with unit Prandtl Number. Since the fluid layer was assumed to have a free surface, the penetration was taken as zero implying $c = 1$.

(c) Boundary layer type flow with combined wall curvature and heating

$$f(y) = y(2-y) \qquad 0 \leq \xi \leq \frac{1}{c}$$

$$f(y) = xy(2-y) + 1 - \chi \qquad \frac{1}{c} \leq \xi \leq 1$$

The same mean temperature profile was assumed except that x was taken as one for the velocity profile and three for the temperature profile. This served to demonstrate the generality of the method while also approximating a possibly real situation in the atmosphere. A value of 0.7 for the Prandtl Number was used in evaluating this case. A semiempirical adjustment for this was made in evaluating the integral Y^o_{mn} by defining a new variable $\xi_1 = \xi \, Pr^{1/3}$ according to Eckert and Drake (19). Hence, when the integration of ξ is carried over the range 0 to 1 , the entire thermal profile is integrated across simultaneously.

(d) Stationary layer of fluid with strongly non-linear temperature profile

$$T_* = y - N_s y(y-1) \qquad 0 \le \xi \le \frac{1}{c}$$

$$T_* = -\chi y \qquad \frac{1}{c} \le \xi \le 1$$

with $\chi = 0.5$ and $N_s = 40$.

This profile is one proposed by Sparrow, Goldstein and Jonsson (20) as being indicative of internally distributed heat sources. However, such a profile is not uncommon in the lower layers of the atmosphere, where the release of latent heat would generate non-linear temperature distributions. As stated above, the unstable layer is capped by fluid of moderate stability. The results to be presented later indicate strongly penetrative convection.

(e) Stationary layer of fluid with parabolic thermal profile posed as a problem in penetrative convection in this example:

$$T_* = y(2-y) \qquad 0 \le \xi \le \frac{1}{c}$$

$$T_* = \frac{1}{(c-1)^2}\,[y(2-y) - c(2-c)] \qquad \frac{1}{c} \le \xi \le 1$$

IV. Discussion of Results

The cases for which the critical conditions were evaluated have been listed earlier, however, in order to facilitate easy comparison they are listed in Table 1 together with the corresponding results.

TABLE 1

	Mean Velocity Profile	Mean Temperature Profile	C_{cr}	Φ_{cr}	Ra_{cr}	$N_{G_{cr}}$
Case (a)	Pohlhausen	Pohlhausen	2.2325	2.9265	735.9	--
		Linear	2.0263	2.7119	311.1	--
Case (b)	Parabolic	Linear	1.0	2.656	--	--
Case (c)	See Table II					
Case (d)	--	Nonlinear	2.1362	2.9447	15.2173	--
Case (e)	--	Parabolic	1.2325	2.71	997.8	--

The first case examined, viz., the boundary layer on a heated flat plate is relevant to the transition mechanism due to thermal stratification effects. An examination of the dimensionless disturbance velocity components in Fig. (2) provide a measure of the degree of penetration of the longitudinal vortices into the freestream. This penetrative action of the vortices has been experimentally observed by Sparrow and Husar (10). The critical Rayleigh numbers have been calculated to be approximately 736 for the Pohlhausen profile and 311 for the linear profile and are listed for convenience in Table II. The point of first instability is therefore highly dependent on the shape of the profile in the unstable layer. Since the system of equations (4) to (8) are coupled in only a linear manner, the onset of convective instability is independent of the shear, a result that is also stated by Gage and Reid (17). (The effect of the shear is only to cause the appearance of the longitudinal rolls without which stationary Bénard type convection occurs). The Pohlhausen temperature profile causes stronger penetration than the linear one, although the latter profile is more unstable.

The penetrative character of the disturbances causes a marked reduction in the critical Rayleigh Number. This may be appreciated by comparing the classical non-penetrative result of $Ra = 1100$ with the result obtained here of 311.1. This value of the critical Rayleigh Number obtained does not agree with those of Rintel (12). A closer examination of his work indicated that he had drawn an incorrect analogy between the narrow gap Taylor problem and the Bénard problem. Such an analogy follows only when the mean temperature profile is linear and continuous throughout the inner and outer (stable) region. Since in fact, the values in his Table II (12) were arrived at by integrating over a region with a discontinuity in the mean thermal profile they are incorrect except for the limiting case with $c = 1$ and $\chi = \infty$ since then the discontinuity ceases to exist.

It should be noted that the eigenfunctions for the temperature and horizontal velocity perturbations are identical when the mean thermal and velocity profiles are the same with Prandtl Number equal one, but different otherwise.

Figure (3) illustrates the results obtained for case (b), i.e., the stability of a parallel free surface flow along a curved heated wall with zero penetration. The analogy between curvature and buoyancy is well displayed in Fig. (4) which is a composite neutral stability curve obtained by plotting Φ , the disturbance wavenumber versus $N_G^2 + \kappa Ra$. This result was arrived at as follows: A previous simple analyses by the authors, of curved flows with thermal stratification, had yielded the parameter $N_G^2 + Ra$ as a stability criterion for linear profiles. It was, therefore, intuitively expected that non-linear profiles would perhaps yield the slightly more general parameter $N_G^2 + \kappa Ra$ where κ now, would account for the differences between the thermal and velocity profiles. Consequently, a number of calculations of the stability boundaries for various values of the parameter R_n were performed. It was then easy to calculate κ and establish that $N_G^2 + \kappa Ra$ was indeed a unique parameter by checking several points on the calculated curves.

A secondary dependence of κ would be on the degree of penetration into the stable fluid, a limiting factor in establishing this dependence being the computer time available. To examine this effect, a small number of calculations were run on case (c) and the critical values obtained in a first approximation in the minimization are given in Table II.

TABLE II

$N_{G_{cr}}$	R_n	Ra	Φ_{cr}	C_{cr}	κ
21.76	0	0.0	2.6943	1.4512	--
11.57	4	536.23	2.7123	1.356	0.633
8.83	8	623.35	2.7153	1.344	0.634

Since the deviation in κ is not large it appears that the same type of relation holds so that one may write $N_{G_{cr}}^2 = N_{G_{cr}}^2\big|_{Ra = 0} - \kappa Ra$.

The difference in the first value of c is probably due to the absence of Prandtl Number effects. The eigenfunctions obtained are plotted in Fig. (5) together with the eigenfunctions of the second modal instability with $Pr = 1$. The neutral stability curves for $R_n = 5$

and 10 and $Pr = 1$ are plotted in Fig. (6). They are, of course, scaled with the critical value of c. Figure (7) contains curves of the variation of critical Goertler Number with Rayleigh Number at the point of first instability.

The results evaluated for cases (d) and (e) are displayed in Figs. (8) and (9). The eigenfunctions drawn in Fig. (8) indicate the passage of the peak of the perturbations into the stable layer. The high value of the penetration coefficient and the extremely low value of the critical Rayleigh Number serve as reminders of the strongly unstable nature of the nonlinear thermal profiles. Therefore, it may be easily appreciated that such nonlinear profiles in the atmosphere (caused perhaps by latent heat release) could give rise to strongly penetrative disturbances resulting in considerable enhancement of the vertical transport of heat, momentum and moisture.

V. Conclusions

The object of this analysis was to explore the stability of parallel layers of fluid under the simultaneous influence of curvature and heating. The simple linear theory indicates not surprisingly, that the two effects are additive, demonstrating the close analogy between streamline curvature and buoyancy. A similar result has been obtained for the case of Thermohaline Convection by Lindberg (21) who arrives at the conclusion that the thermal Rayleigh Number and an analogously defined "Concentration Rayleigh Number" add linearly to form a stability parameter. The stability of a few nonlinear temperature profiles was investigated and their strongly penetrative nature demonstrated. Since such profiles are not uncommon in the atmosphere, it is reasonable to expect that convective instabilities could be generated in the lower layers, causing considerable modification of the vertical transport of heat, moisture and momentum, as is stated by Estoque (13).

Future work should include the interaction of the Tollmein Schlichting wave instabilities with truly three dimensional convective disturbances. The disturbances analyzed here have been quasi-two-dimensional in that no variations in the streamwise direction have been assumed. The behavior of penetrative instabilities in an Ekman layer flow should also prove interesting since this approximates more closely the true atmospheric situation. Finally, the need for some simple nonlinear analyses to establish the interaction mechanism between the disturbances and the mean flow is now becoming of vital necessity.

VI. References

1. Taylor, G. I., "Stability of a viscous liquid contained between two rotating cylinders," Phil. Trans. of Royal Soc., (1923).

2. Goertler, H., "On the three dimensional instability of laminar boundary layers on concave walls," NACA TM 1375, (1954).

3. Smith, A.M.O., "On the growth of Taylor Goertler vortices along highly concave walls," Quart. of Applied Math., Vol. 3, No. 3, pp. 233-262, (1955).

4. Liepmann, H. W., "Investigations on laminar boundary-layer stability and transition on curved boundaries," NACA ACR No. 3H30, (1943).

5. Tani, Itiro, "Production of longitudinal vortices in the boundary-layer along a concave wall," Jour. of Geophysical Research, Vol. 67, No. 8, (July 1962).

6. Goertler, H., "Uber eine Analogie zwischen den Instabilitaten Laminarer Grenzschichtstromungen an Konkaven Wanden und an erwarmten Wanden," Ing. Arch., Vol. 28, (1959).

7. Yih, C. S., "Dynamics of non-homogeneous fluids," Macmillan Press, (1965).

8. Bradshaw, P., "The analogy between streamline curvature and buoyancy in turbulent shear flow," J.F.M., Vol. 36, Pt. 1, p. 177.

9. Terada, "Some experiments on Periodic columnar forms of vortices caused by convection," Tokyo Imperial University Research Report No. 31, (January 1928).

10. Sparrow, E. M. and Husar, R. B., "Longitudinal vortices in natural convection flow on Inclined plates," J.F.M. Vol. 37, Pt. 2, p. 251, (1969).

11. Kuettner, J., "The band structure of the atmosphere," Tellus Vol. 11, No. 3, p. 267, (1959).

12. Kuo, H. L., "Perturbations of plane Couette flow in stratified fluid and origin of cloud streets," Phys. of Fluids, Vol. 6, No. 2, p. 195, (1963).

13. Estoque, M. A., "Vertical mixing due to penetrative convection," Jour. of Atm. Sci., Vol.25, No. 6, p. 1046, (November 1968).

14. Stix, M., "Two examples of penetrative convection," Tellus Vol. 22, No. 5, p. 517, (1970).

15. Whitehead, J. A. and Chen, M. M., "Thermal instability and convection of a thin fluid layer bonded by a stably stratified region," Jour. of Fluid Mech., Vol. 40, Pt. 3, p. 549, (1970).

16. Rintel, L., "Penetrative convective instabilities," Phys. of Fluids, Vol. 10, No. 4, p. 848, (April 1967).

17. Gage, K. S. and Reid, W. H., " The stability of thermally stratified plane Poiseuille flow," J.F.M. Vol. 33, Pt. 1, p. 21, (1968).

18. Chandrasekhar, S., "Hydrodynamic and hydromagnetic stability," Oxford University Press, (1961).

19. Eckert, E.R.G. and Drake, R.M., "Heat and mass transfer," 2nd edition, McGraw-Hill, (1959).

20. Sparrow, E. M., Goldstein, R. J., and Johnson, V. K., "Thermal instability in a horizontal fluid layer: Effect of boundary conditions and nonlinear temperature profile," J.F.M. Vol. 18, Pt. 4, p. 513, (April 1964).

21. Lindberg, W., "Theoretical aspects of thermohaline convection," Ph.D. dissertation, Colorado State University, Fort Collins, Colorado, (1970).

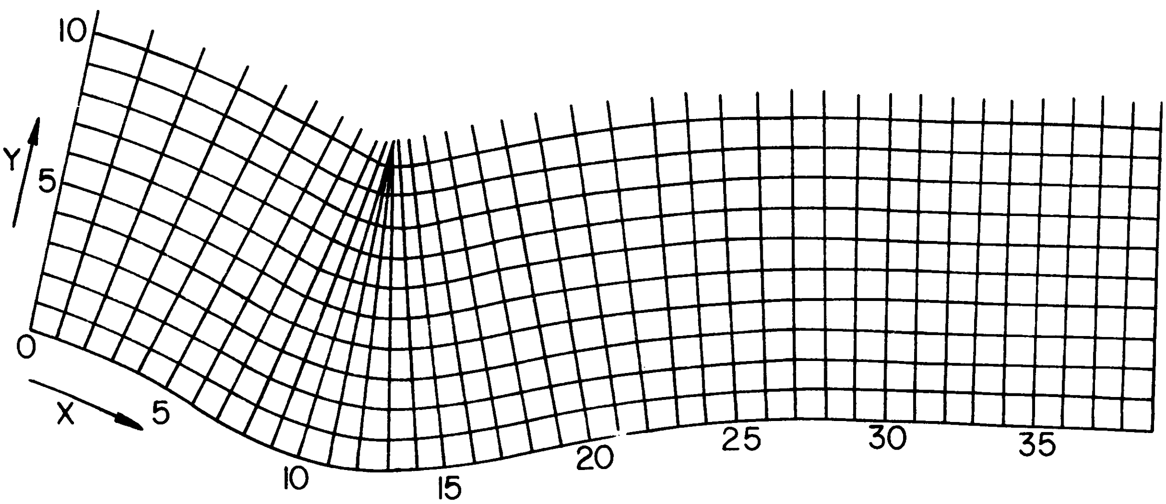

a - A Family of Parallel Curves

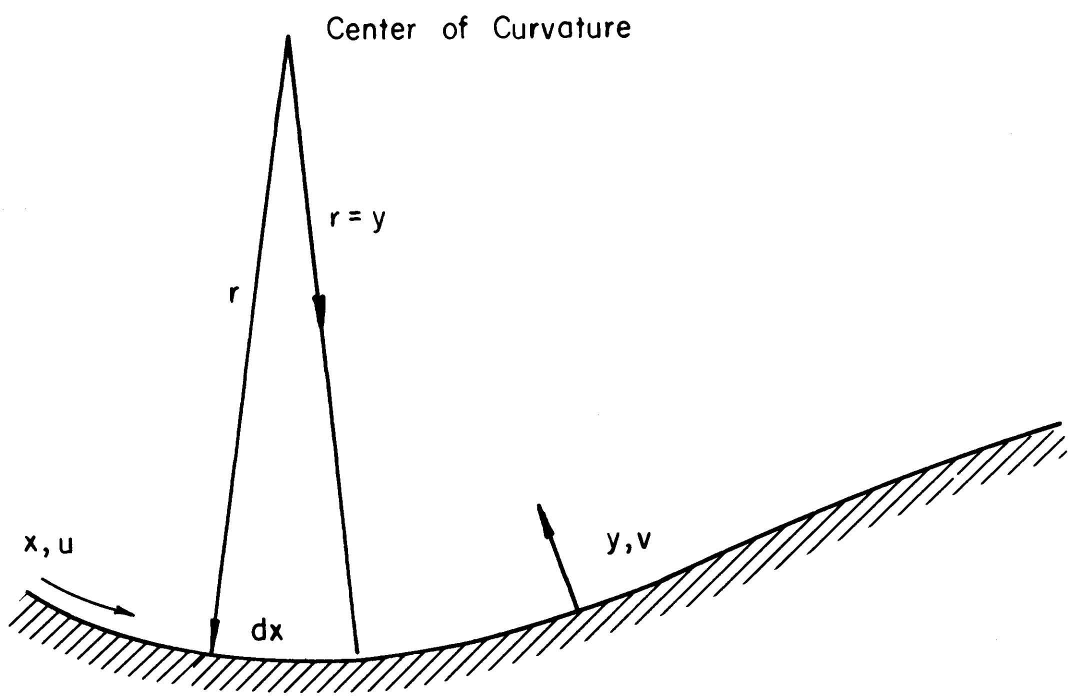

b - Dimensional Relationships

Fig. 1 Orthogonal Curvilinear Coordinate System

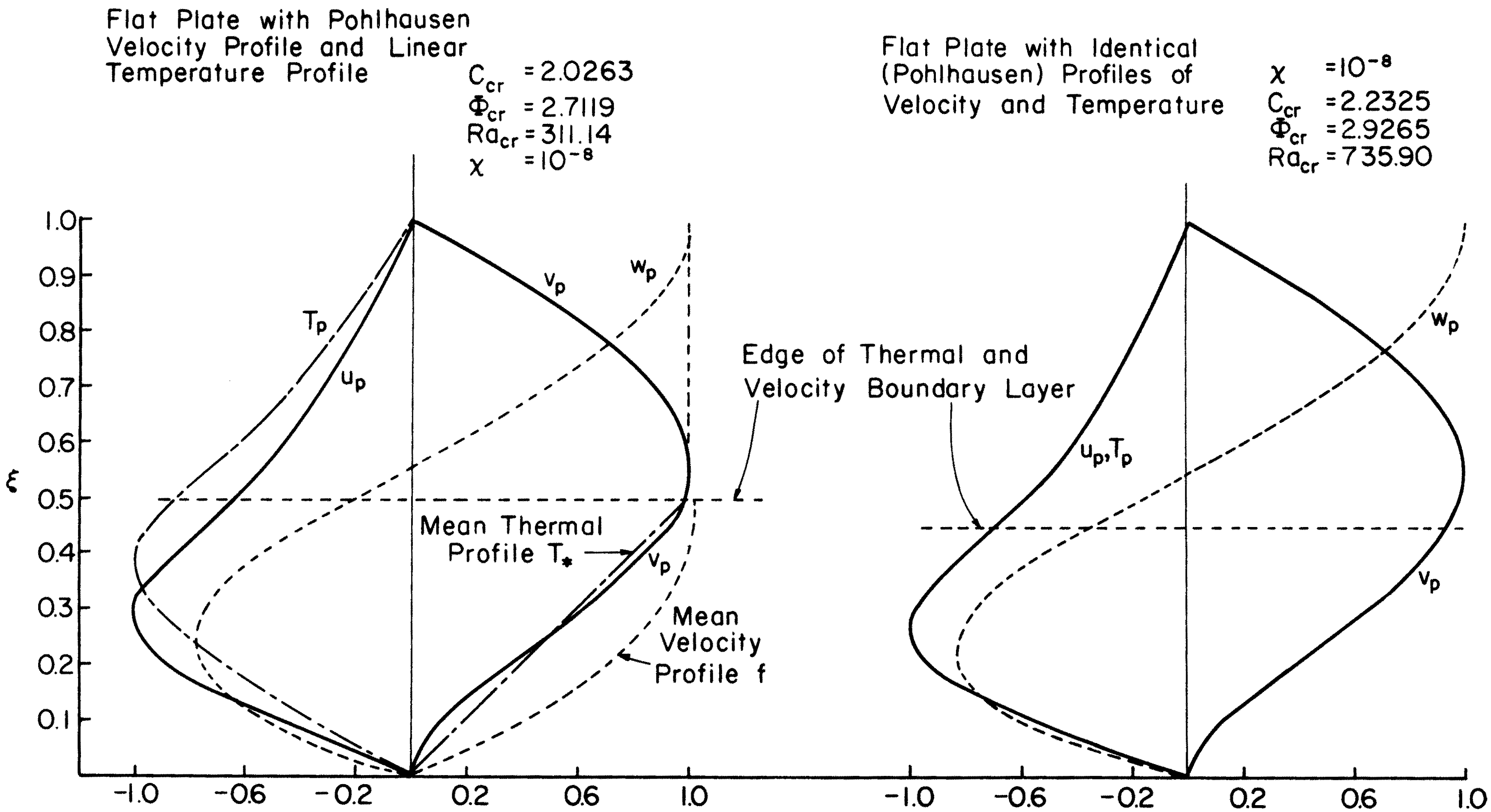

Figure 2. Perturbation Components for Case (a) Prandtl Number = 1

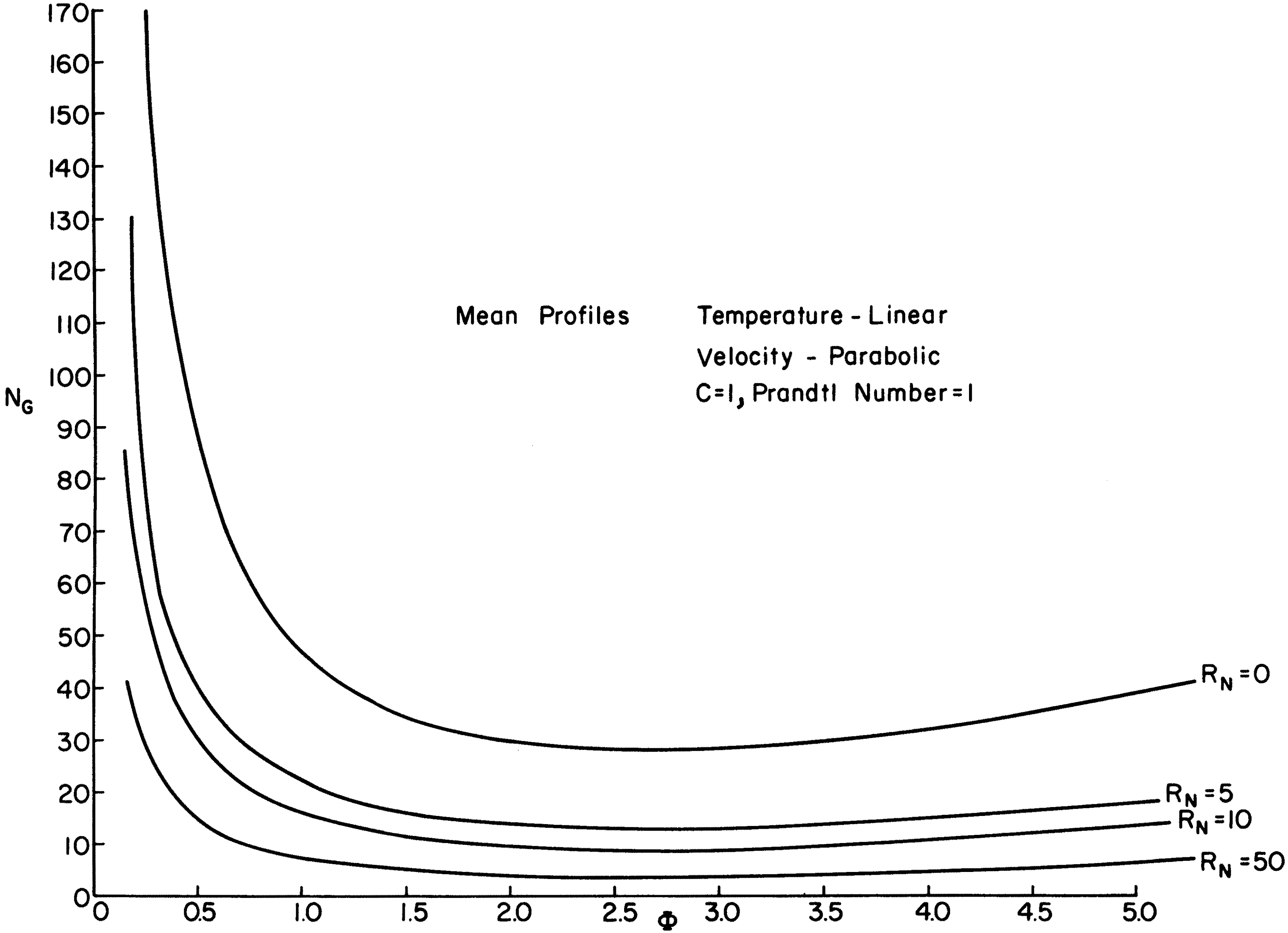

Figure 3. Case (b) Plot of Goertler Number vs. Wavenumber for Different R_N

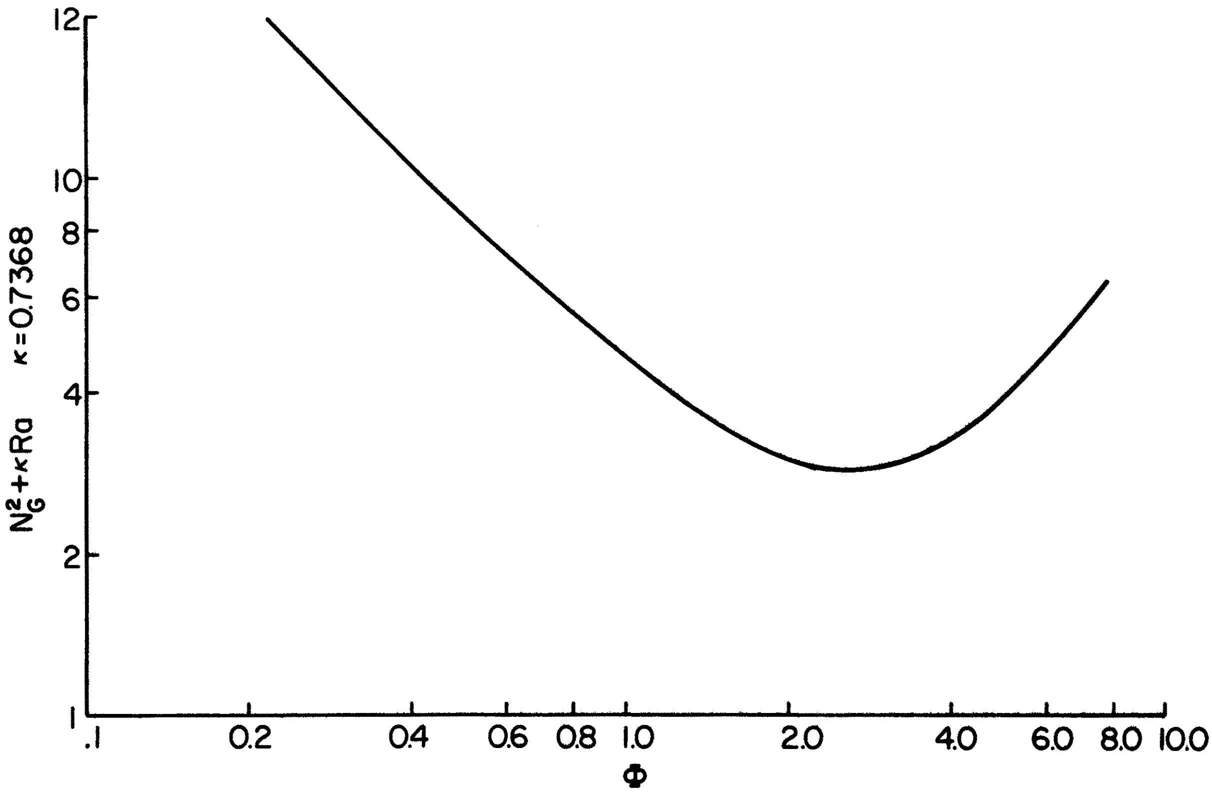

Figure 4. Case (b) Neutral Stability Curve $\kappa = 0.7368$

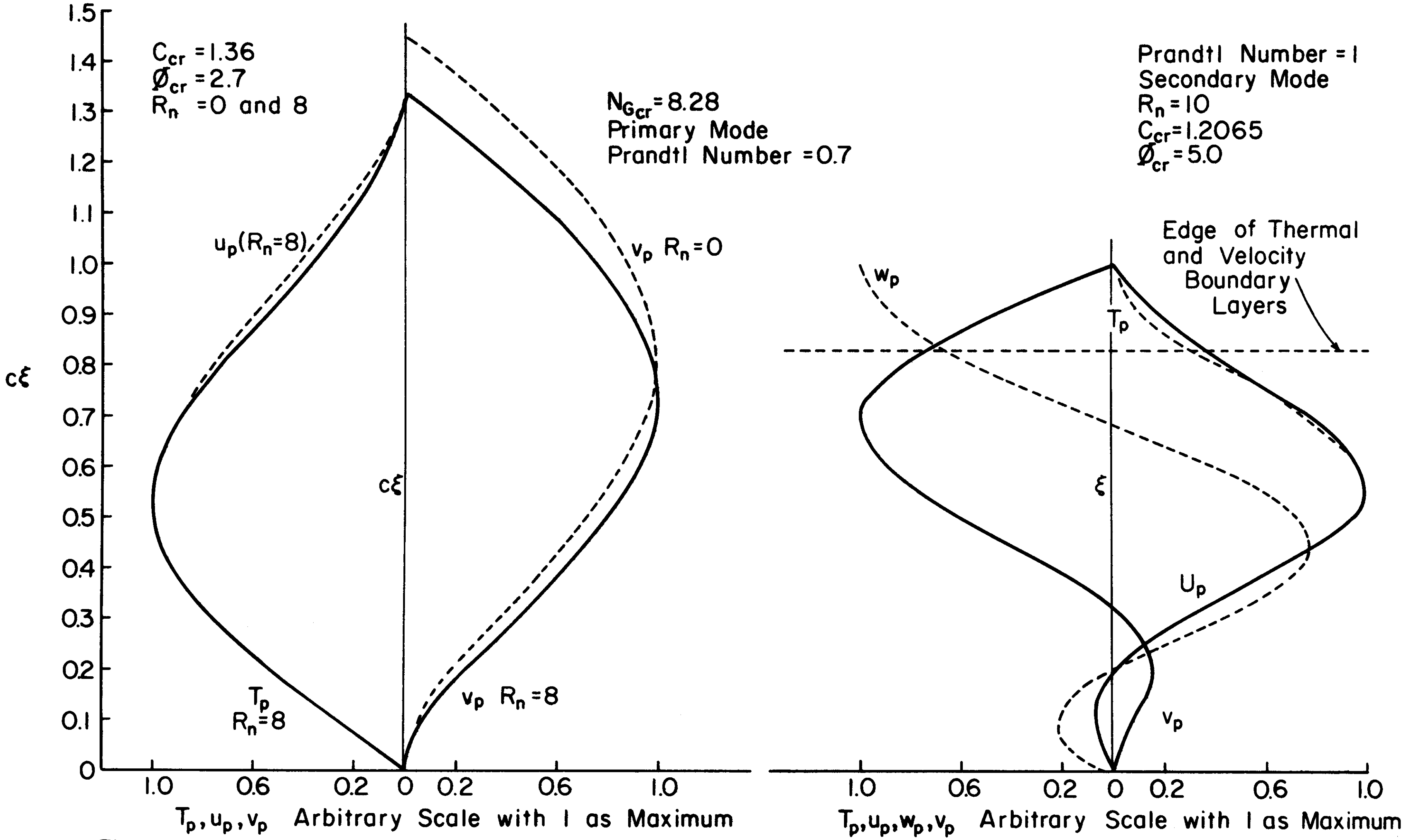

Figure 5. Examples of Velocity and Temperature Perturbations Obtained for Case (c)

$\chi = 1.0$ (Velocity Profile)

$\chi = 3.0$ (Temperature Profile)

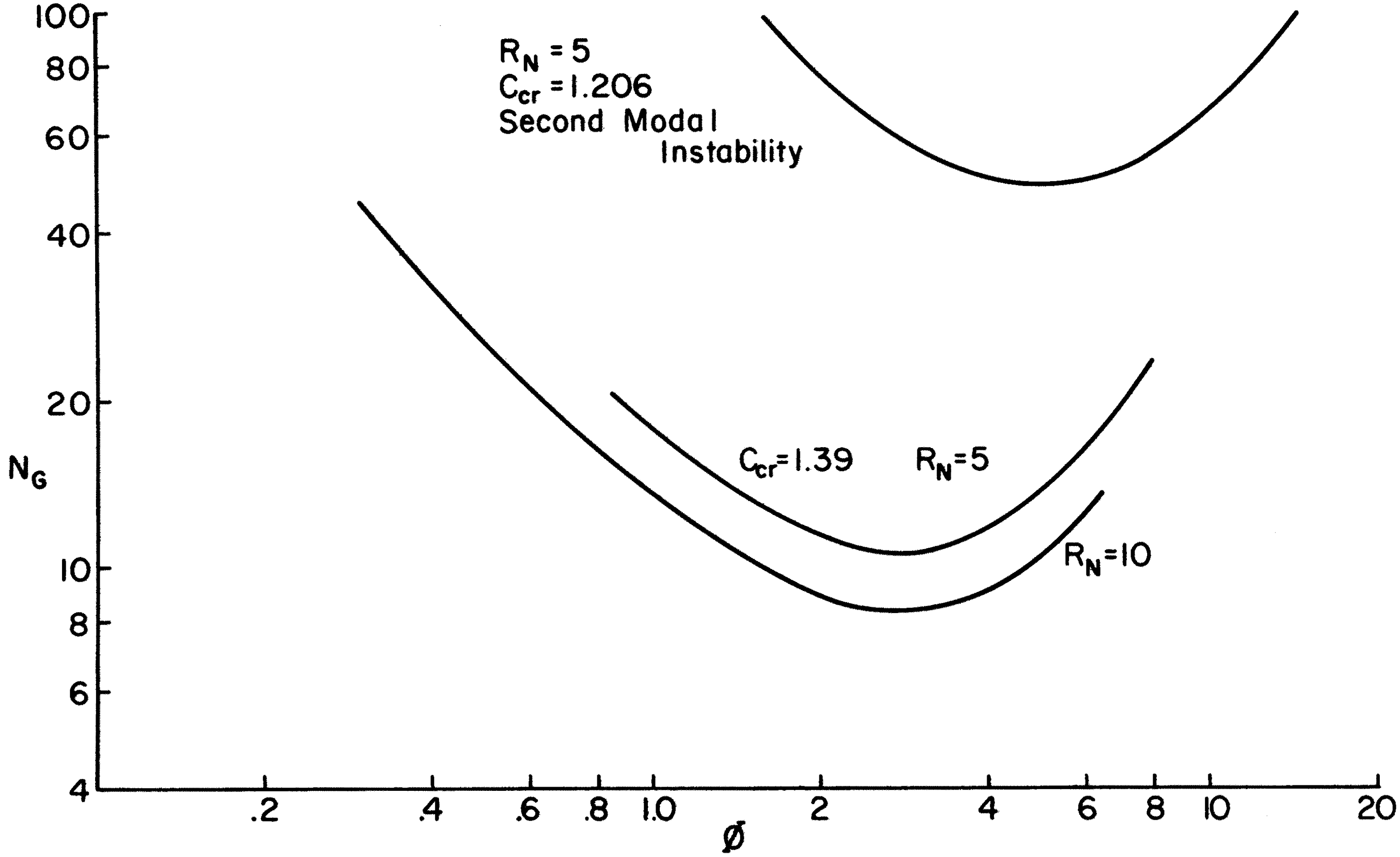

Figure 6. Neutral Stability Curves for Case (c). The Critical Conditions for the Primary and Secondary Mode are Indicated.

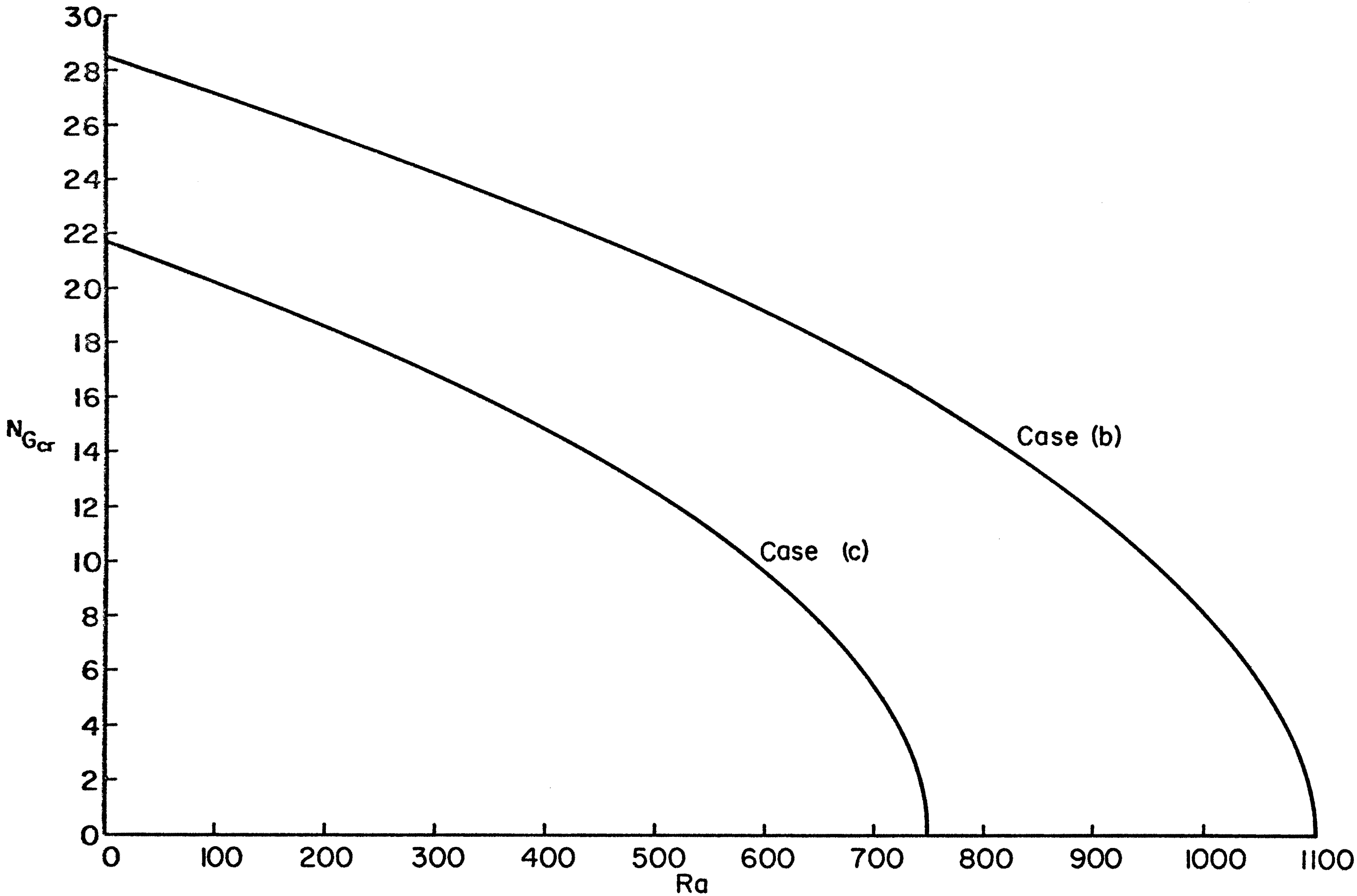

Figure 7. Variation of Critical Goertler Number with Rayleigh Number for Cases (b) and (c)

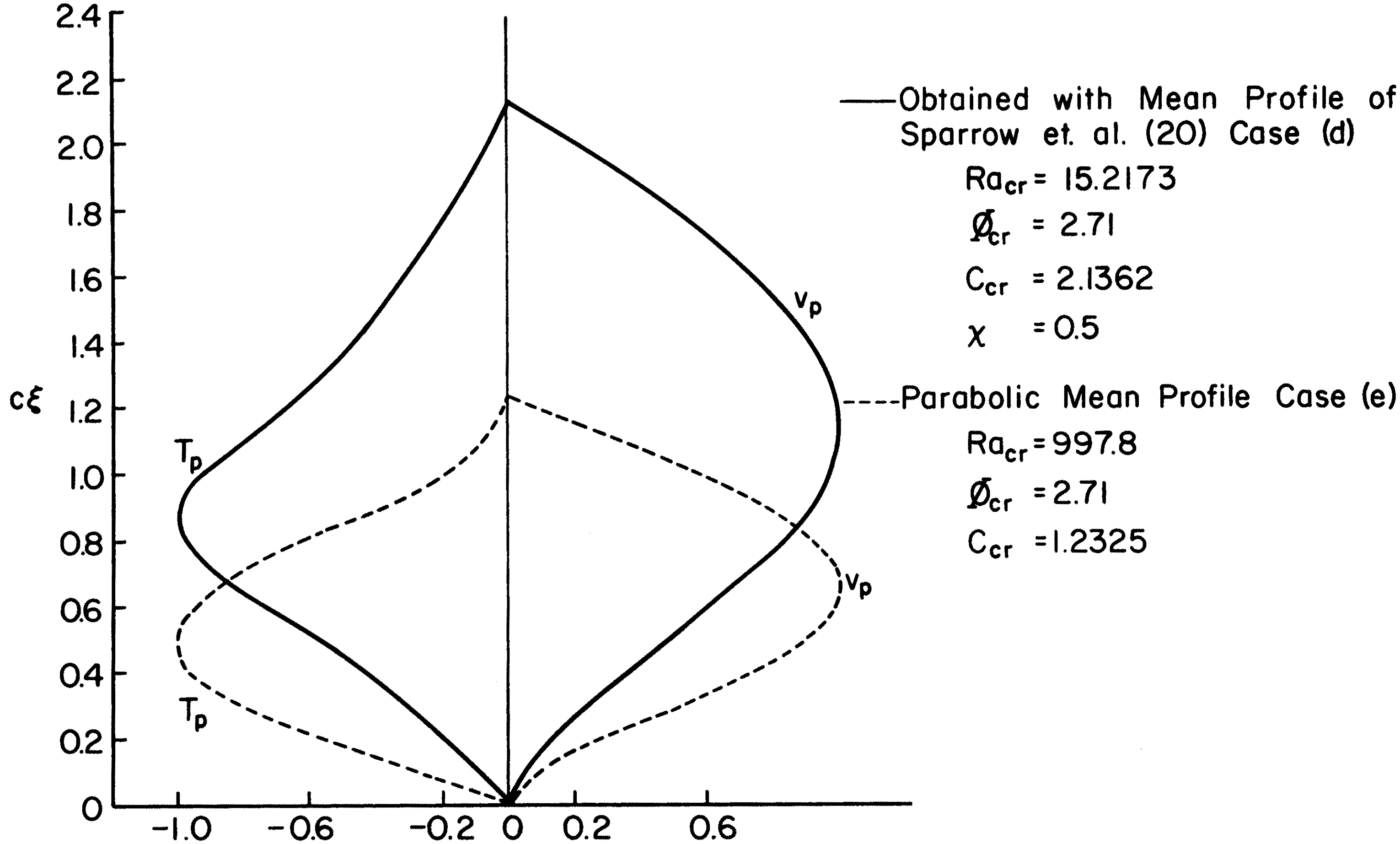

Figure 8. Temperature and Vertical Velocity Perturbations obtained for Cases (d) and (e)

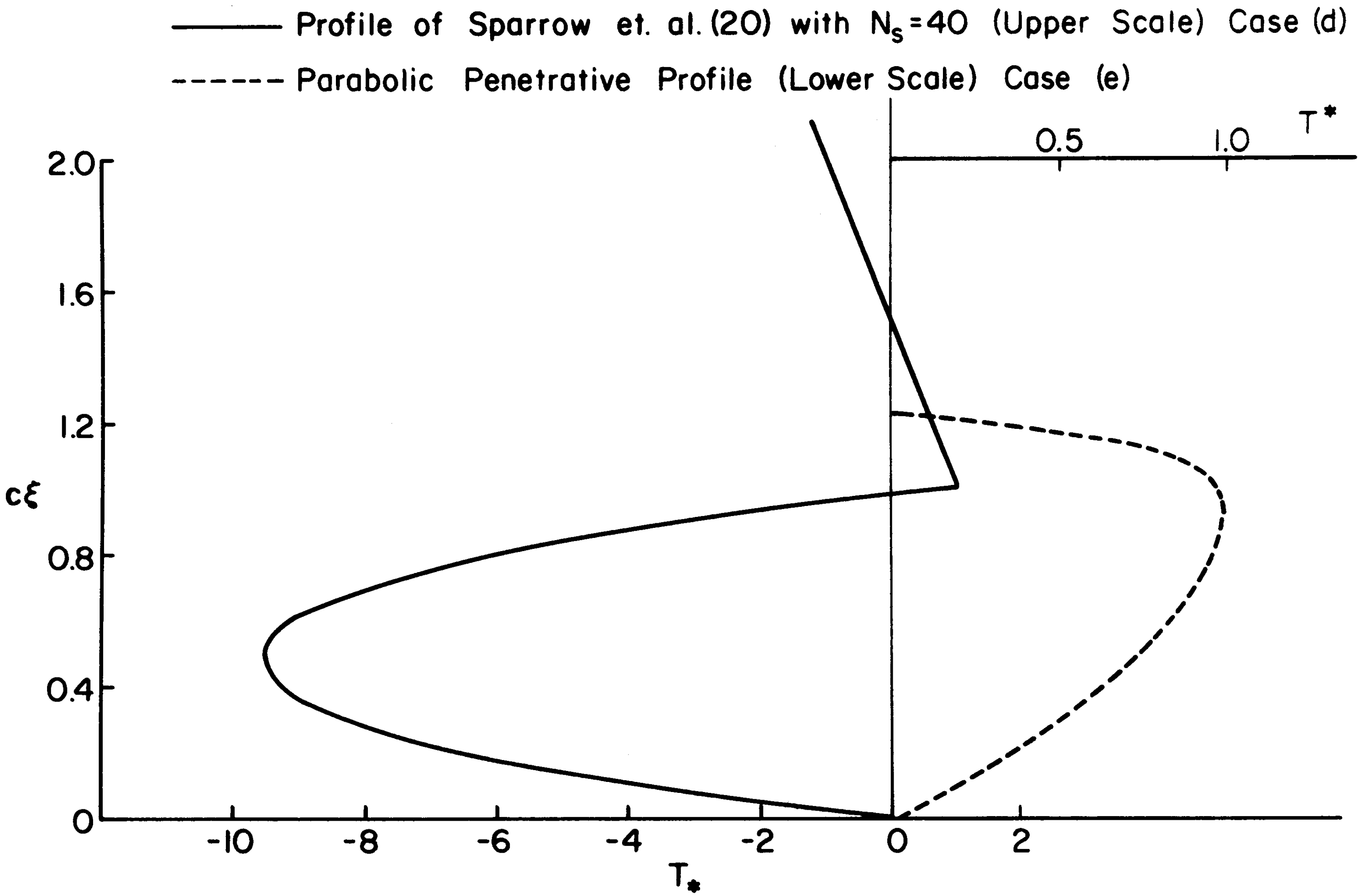

Figure 9. Mean Temperature Profiles for Cases (d) and (e)

unclassified

Security Classification

DOCUMENT CONTROL DATA - R & D

(Security classification of title, body of abstract and indexing annotation must be entered when the overall report is classified)

1. ORIGINATING ACTIVITY *(Corporate author)*

Fluid Dynamics & Diffusion Laboratory
College of Engineering, Colorado State University
Fort Collins, Colorado 80521

2a. REPORT SECURITY CLASSIFICATION

Unclassified

2b. GROUP

3. REPORT TITLE

Penetrative Convective Instabilities in Parallel Flows

4. DESCRIPTIVE NOTES *(Type of report and inclusive dates)*

Technical Report

5. AUTHOR(S) *(First name, middle initial, last name)*

Rene A. Kahawita and Robert N. Meroney

6. REPORT DATE	7a. TOTAL NO. OF PAGES	7b. NO. OF REFS
May 1972	29	21

8a. CONTRACT OR GRANT NO.

14-01-0001

b. PROJECT NO.

N00014-68-A-0493-0001

c.

d.

9a. ORIGINATOR'S REPORT NUMBER(S)

CER71-72RK-RNM-24

9b. OTHER REPORT NO(S) *(Any other numbers that may be assigned this report)*

10. DISTRIBUTION STATEMENT

Distribution of this report is unlimited.

11. SUPPLEMENTARY NOTES

12. SPONSORING MILITARY ACTIVITY

U.S. Department of Defense
Office of Naval Research

13. ABSTRACT

An analysis has been performed of penetrative convective instabilities arising from the combined action of thermal and centrifugal buoyancy forces. The theory allows for the fact that in the atmosphere, convection arising in an unstable layer may penetrate into a neighboring stable region. The objective has been to examine the effect of various mean temperature and velocity profiles on the critical limit and convective penetration of the distrubances. The linearized perturbation equations have been solved employing an approximate technique. The results obtained indicate that nonlinear profiles are more unstable and penetrative than linear ones. The close analogy between streamline curvature and thermal stratification effects has been demonstrated. It is found that for parallel layers of fluid along curved heated walls, a unique stability curve for neutral disturbances may be obtained if the quantity plotted along the abscissa is $Ra + \kappa N_G^2$ where Ra is the Rayleigh Number, N_G is the Goertler Number and κ a constant which expresses the relative importance of the mean temperature and velocity profiles.

DD FORM 1 NOV 65 1473

Unclassified

Security Classification

14 KEY WORDS	LINK A		LINK B		LINK C	
	ROLE	WT	ROLE	WT	ROLE	WT
Boundary Layer Instability						
Penetrative Convection						
Convective Instabilities						
Goertler Instability						
Rayleigh Convection						
Thermal Instability						

DISTRIBUTION LIST FOR UNCLASSIFIED
TECHNICAL REPORTS ISSUED UNDER
CONTRACT N00014-68-A 0493-0001 TASK 000-414

Defense Documentation Center
Cameron Station
Alexandria, Virginia 22314 (12)

Technical Library
Naval Ship Research and Development Laboratory
Annapolis, Maryland 21402

Professor Bruce Johnson
Engineering Department
Naval Academy
Annapolis, Maryland 21402

Library
Naval Academy
Annapolis, Maryland 21402

Professor W.R. Debler
Department of Engineering Mechanics
University of Michigan
Ann Arbor, Michigan 48108

Professor W.P. Graebel
Department of Engineering Mechanics
University of Michigan
College of Engineering
Ann Arbor, Michigan 48108

Professor Finn C. Michelsen
Naval Architecture and Marine Engineering
445 West Engineering Building
University of Michigan
Ann Arbor, Michigan 48108

Dr. Francis Ogilvie
Department of Naval Architecture and Marine Engineering
University of Michigan
Ann Arbor, Michigan 48108

Professor W.W. Willmarth
Department of Aerospace Engineering
University of Michigan
Ann Arbor, Michigan 48108

Dr. S.A. Piacsek
Argonne National Laboratory
Applied Mathematics Division
9700 S. Cass Avenue
Argonne, Illinois 60439

AFOSR (REM)
1400 Wilson Boulevard
Arlington, Virginia 22204

Professor S. Corrsin
Mechanics Department
The Johns Hopkins University
Baltimore, Maryland 20910

Professor L.S.G. Kovasznay
The Johns Hopkins University
Baltimore, Maryland 20910

Professor O.M. Phillips
The Johns Hopkins University
Baltimore, Maryland 20910

Librarian
Department of Naval Architecture
University of California
Berkeley, California 94720

Professor Israel Cornet
Department of Mechanical Engineering
University of California
Berkeley, California 94720

Professor M. Holt
Division of Aeronautical Sciences
University of California
Berkeley, California 94720

Professor E.V. Laitone
Department of Mechanical Engineering
University of California
Berkeley, California 94720

Professor P. Lieber
Department of Mechanical Engineering
University of California
Institute of Engineering Research
Berkeley, California 94720

Professor J.R. Paulling
Department of Naval Architecture
University of California
Berkeley, California 94720

Professor J.V. Wehausen
Department of Naval Architecture
University of California
Berkeley, California 94720

Professor E.R. van Driest
Virginia Polytechnic Institute and University
Department of Aerospace Engineering
Blacksburg, Virginia 24061

Commander
Boston Naval Shipyard
Boston, Massachusetts 02129

Director
Office of Naval Research Branch Office
495 Summer Street
Boston, Massachusetts 02210

Commander
Puget Sound Naval Shipyard
Bremerton, Washington 98314

Professor J.J. Foody
Chairman, Engineering Department
State University of New York
Maritime College
Bronx, New York 10465

Dr. Alfred Ritter
Assistant Head, Applied Mechanics Department
Cornell Aeronautical Laboratory, Inc.
Buffalo, New York 14221

Dr. J.W. Morris
Manager, Material Sciences Section
Advanced Materials Research
Bell Aerospace Company
P.O. Box 1
Buffalo, New York 14240

Professor G.H. Carrier
Department of Engineering and Applied Physics
Harvard University
Cambridge, Massachusetts 02138

Commanding Officer
NROTC Naval Administrative Unit
Massachusetts Institute of Technology
Cambridge, Massachusetts 02139

Professor M.A. Abkowitz
Department of Naval Architecture and Marine Engineering
Massachusetts Institute of Technology
Cambridge, Massachusetts 02139

Professor A.T. Ippen
Department of Civil Engineering
Massachusetts Institute of Technology
Cambridge, Massachusetts 02139

Professor L.N. Howard
Department of Mathematics
Massachusetts Institute of Technology
Cambridge, Massachusetts 02139

Professor E.W. Merrill
Department of Mathematics
Massachusetts Institute of Technology
Cambridge, Massachusetts 02139

Professor E. Mollo-Christensen
Room 54-1722
Massachusetts Institute of Technology
Cambridge, Massachusetts 02139

Professor N. Newman
Department of Naval Architecture and Marine Engineering
Massachusetts Institute of Technology
Cambridge, Massachusetts 02139

Professor A.H. Shapiro
Department of Mechanical Engineering
Massachusetts Institute of Technology
Cambridge, Massachusetts 02139

Commander
Charleston Naval Shipyard
U.S. Naval Base
Charleston, South Carolina 29408

A.R. Kuhlthau, Director
Research Laboratories for the Engineering Sciences
Thorton Hall, University of Virginia
Charlottesville, Virginia 22903

Director
Office of Naval Research Branch Office
536 South Clark Street
Chicago, Illinois 60605

Library
Naval Weapons Center
China Lake, California 93555

Professor J.M. Burgers
Institute of Fluid Dynamics and Applied Mathematics
University of Maryland
College Park, Maryland 20742

Professor Pai
Institute for Fluid Dynamics and Applied Mathematics
University of Maryland
College Park, Maryland 20740

Acquisition Director
NASA Scientific & Technical Information
P.O. Box 33
College Park, Maryland 20740

Technical Library
Naval Weapons Laboratory
Dahlgren, Virginia 22448

Computation & Analyses Laboratory
Naval Weapons Laboratory
Dahlgren, Virginia 22448

Dr. C.S. Wells, Jr.
Manager - Fluid Mechanics
Advanced Technology Center, Inc.
P.O. Box 6144
Dallas, Texas 75222

Dr. R.H. Kraichnan
Dublin, New Hampshire 03444

Commanding Officer
Army Research Office
Box CM, Duke Station
Durham, North Carolina 27706

Professor A. Charnes
The Technological Institute
Northwestern University
Evanston, Illinois 60201

Dr. Martin H. Bloom
Polytechnic Institute of Brooklyn
Graduate Center, Dept. of Aerospace
Engineering and Applied Mechanics
Farmingdale, New York 11735

Technical Documents Center
Building 315
U.S. Army Mobility Equipment
Research and Development Center
Fort Belvoir, Virginia 22060

Professor J.E. Cermak
College of Engineering
Colorado State University
Ft. Collins, Colorado 80521

Technical Library
Webb Institute of Naval Architecture
Glen Cove, Long Island, New York 11542

Professor E.V. Lewis
Webb Institute of Naval Architecture
Glen Cove, Long Island, New York 11542

Dr. B.N. Pridmore Brown
Northrop Corporation
NORAIR-Div.
Hawthorne, California 90250

Dr. J.P. Breslin
Stevens Institute of Technology
Davidson Laboratory
Hoboken, New Jersey 07030

Dr. D. Savitsky
Stevens Institute of Technology
Davidson Laboratory
Hoboken, New Jersey 07030

Mr. C.H. Henry
Stevens Institute of Technology
Davidson Laboratory
Hoboken, New Jersey 07030

Dr. J.P. Craven
University of Hawaii
1801 University Avenue
Honolulu, Hawaii 96822

Professor E.L. Resler
Graduate School of Aeronautical Engineering
Cornell University
Ithaca, New York 14851

Professor John Miles
c/o I.G.P.P.
University of California, San Diego
La Jolla, California 92038

Director
Scrippe Institution of Oceanography
University of California
La Jolla, California 92037

Professor A. Ellis
University of California, San Diego
Department of Aerospace & Mechanical Engineering
La Jolla, California 92037

Dr. B. Sternlicht
Mechanical Technology Incorporated
968 Albany-Shaker Road
Latham, New York 12110

Dr. Coda Pan
Mechanical Technology Incorporated
968 Albany-Shaker Road
Latham, New York 12110

Mr. P. Eisenberg, President
Hydronautics, Inc.
Pindell School Road
Howard County
Laurel, Maryland 20810

Mr. M.P. Tulin
Hydronautics, Inc.
Pindell School Road
Howard County
Laurel, Maryland 20810

Mr. Alfonso Alcedan L.,Director
Laboratorio Nacional De Hydraulics
Antigui Cameno A. Ancon
Casilla Jostal 682
Lima, Peru

Commander
Long Beach Naval Shipyard
Long Beach, California 90802

Professor John Laufer
Department of Aerospace Engineering
University Park
Los Angeles, California 90007

Professor J.M. Killen
St. Anthony Falls Hydraulic Lab.
University of Minnesota
Minneapolis, Minnesota 55414

Lorenz G. Straub Library
St. Anthony Falls Hydraulic Lab.
Mississippi River at 3rd Avenue S.E.
Minneapolis, Minnesota 55414

Professor J. Ripkin
St. Anthony Falls Hydraulic Lab.
University of Minnesota
Minneapolis, Minnesota 55414

Dr. W. Silberman
St. Anthony Falls Hydraulic Lab.
Mississippi River at 3rd Avenue S.E.
Minneapolis, Minnesota 55414

Superintendent
Naval Postgraduate School
Library Code 0212
Monterey, California 93940

Professor A.B. Metzner
University of Delaware
Newark, New Jersey 19711

Technical Library
Naval Underwater Systems Center
Newport, Rhode Island 02840

Professor Dudley D. Fuller
Department of Mechanical Engineering
Columbia University
New York, New York 10027

Professor V. Castelli
Department of Mechanical Engineering
Columbia University
New York, New York 10027

Professor H. Elrod
Department of Mechanical Engineering
Columbia University
New York, New York 10027

Professor J.J. Stoker
Institute of Mathematical Sciences
New York University
251 Mercer Street
New York, New York 10003

Society of Naval Architects and Marine Engineering
74 Trinity Place
New York, New York 10006

Engineering Societies Library
345 East 47th Street
New York, New York 10017

Office of Naval Research
New York Area Office
207 W. 24th Street
New York, New York 10011

Miss O.M. Leach, Librarian
National Research Council
Aeronautical Library
Montreal Road
Ottawa 7, Canada

Technical Library
Naval Ship Research and Development Center
Panama City, Florida 32401

Technical Library
Naval Undersea R & D Center
Pasadena Laboratory
3202 E. Foothill Boulevard
Pasadena, California 91107

Dr. Andrew Fabula
Naval Undersea Research & Development Center
Pasadena Laboratory
3202 E. Foothill Boulevard
Pasadena, California 91107

Dr. J.W. Hoyt
Naval Undersea R & D Center
Pasadena Laboratory
3202 E. Foothill Boulevard
Pasadena, California 91107

Professor A. Acosta
Department of Mechanical Engineering
California Institute of Technology
Pasadena, California 91109

Professor H. Liepmann
Department of Aeronautics
California Institute of Technology
Pasadena, California 91109

Professor M.S. Plesset
Engineering Division
California Institute of Technology
Pasadena, California 91109

Professor A. Roshko
California Institute of Technology
Pasadena, California 91109

Professor T.Y. Wu
Department of Engineering
California Institute of Technology
Pasadena, California 91109

Director
Office of Naval Research Branch Office
1030 E. Green Street
Pasadena, California 91101

Naval Ship Engineering Center
Philadelphia Division
Technical Library
Philadelphia, Pennsylvania 19112

Technical Library
Philadelphia Naval Shipyard
Philadelphia, Pennsylvania 19112

Professor R.C. Mac Camy
Department of Mathematics
Carnegie Institute of Technology
Pittsburgh, Pennsylvania 15213

Dr. Paul Kaplan
Oceanics, Inc.
Plainview, Long Island, New York 11803

Technical Library
Naval Missile Center
Point Mugu, California 93441

Technical Library
Naval Civil Engineering Laboratory
Port Hueneme, California 93041

Commander
Portsmouth Naval Shipyard
Portsmouth, New Hampshire 03801

Commander
Norfolk Naval Shipyard
Portsmouth, Virginia 23709

Professor F.E. Bisshopp
Division of Engineering
Brown University
Providence, Rhode Island 02912

Dr. William A. Gross, Vice President
Ampex Corporation
401 Broadway
Redwood City, California 94063

Dr. H.N. Abramson
Southwest Research Institute
8500 Culebra Road
San Antonio, Texas 78228

Editor
Applied Mechanics Review
Southwest Research Institute
8500 Culebra Road
San Antonio, Texas 78206

Office of Naval Research
San Francisco Area Office
50 Fell Street
San Francisco, California 94102

Library
Pearl Harbor Naval Shipyard
Box 400
FPO San Francisco, California 96610

Technical Library
Hunters Point Naval Shipyard
San Francisco, California 94135

Librarian
Naval Ordnance Laboratory
White Oak
Silver Spring, Maryland 20910

Fenton Kennedy Document Library
The Johns Hopkins University
Applied Physics Laboratory
8621 Georgia Avenue
Silver Spring, Maryland 20910

Professor E.Y. Hsu
Department of Civil Engineering
Stanford University
Stanford, California 94305

Dr. Byrne Perry
Department of Civil Engineering
Stanford University
Stanford, California 94305

Dr. R.L. Street
Department of Civil Engineering
Stanford University
Stanford, California 94305

Professor Milton Van Dyke
Department of Aeronautical Engineering
Stanford University
Stanford, California 94305

Professor R.C. Di Prima
Department of Mathematics
Rensselaer Polytechnic Institute
Troy, New York 12180

Professor J. Lumley
Ordnance Research Laboratory
Pennsylvania State University
University Park, Pennsylvania 16801

Dr. M. Sevik
Ordnance Research Laboratory
Pennsylvania State University
University Park, Pennsylvania 16801

Dr. J.M. Robertson
Department of Theoretical and Applied Mechanics
University of Illinois
Urbana, Illinois 61803

Technical Library
Mare Island Naval Shipyard
Vallejo, California 94592

Code 438
Office of Naval Research
Department of the Navy
Arlington, Virginia 22217 (3)

Code 461
Office of Naval Research
Department of the Navy
Arlington, Virginia 22217

Code 463
Office of Naval Research
Department of the Navy
Arlington, Virginia 22217

Code 472
Office of Naval Research
Department of the Navy
Arlington, Virginia 22217

Code 468
Office of Naval Research
Department of the Navy
Arlington, Virginia 22217

Code 473
Office of Naval Research
Department of the Navy
Arlington, Virginia 22217

Code 481
Office of Naval Research
Department of the Navy
Arlington, Virginia 22217

Code 2627
Naval Research Laboratory
Washington, D.C. 20390 (6)

Library, Code 2620 (ONRL)
Naval Research Laboratory
Washington, D.C. 20390 (6)

Code 6170
Naval Research Laboratory
Washington, D.C. 20390

Code 4000
Director of Research
Naval Research Laboratory
Washington, D.C. 20390

Code 8030 (Maury Center)
Naval Research Laboratory
Washington, D.C. 20390

Code 8040
Naval Research Laboratory
Washington, D.C. 20390

Code 031
Naval Ship Systems Command
Washington, D.C. 20390

Code 0341
Naval Ship Systems Command
Washington, D.C. 20390

Code 03412B (L. Benen)
Naval Ship Systems Command
Washington, D.C. 20390

Code 03412 (J. Schuler)
Naval Ship Systems Command
Washington, D.C. 20390

Code 2052
Naval Ship Systems Command
Washington, D. C. 20390

Code 6034
Naval Ship Engineering Center
Center Building
Prince George's Center
Hyattsville, Maryland 20782

Code 6110
Naval Ship Engineering Center
Center Building
Prince George's Center
Hyattsville, Maryland 20782

Code 6113
Naval Ship Engineering Center
Center Building
Prince George's Center
Hyattsville, Maryland 20782

Code 6114
Naval Ship Engineering Center
Center Building
Prince George's Center
Hyattsville, Maryland 20782

Code 6120E
Naval Ship Engineering Center
Center Building
Prince George's Center
Hyattsville, Maryland 20782

Code 6136
Naval Ship Engineering Center
Center Building
Prince George's Center
Hyattsville, Maryland 20782

Dr. A. Powell
Code 01
Naval Ship Research and Development Center
Washington, D.C. 20034

Mr. W.M. Ellsworth
Code OH50
Naval Ship Research and Development Center
Washington, D.C. 20034

Central Library
Code L42
Naval Ship Research and Development Center
Washington, D.C. 20034

Dr. W.E. Cummins
Code 500
Naval Ship Research and Development Center
Washington, D.C. 20034

Mr. S.F. Crump
Code 513
Naval Ship Research and Development Center
Washington, D.C. 20034

Mr. R. Wermter
Code 520
Naval Ship Research and Development Center
Washington, D.C. 20034

Dr. P. Pien
Code 521
Naval Ship Research and Development Center
Washington, D.C. 20034

Dr. W.B. Morgan
Code 540
Naval Ship Research and Development Center
Washington, D.C. 20034

Mr. P. Granville
Code 541
Naval Ship Research and Development Center
Washington, D.C. 20034

Mr. J.B. Hadler
Code 560
Naval Ship Research and Development Center
Washington, D.C. 20034

Dr. H.R. Chaplin
Code 600
Naval Ship Research and Development Center
Washington, D.C. 20034

Mr. G.H. Gleissner
Code 800
Naval Ship Research and Development Center
Washington, D.C. 20034

Dr. M. Strasberg
Code 901
Naval Ship Research and Development Center
Washington, D.C. 20034

Mr. J. McCarthy
Code 552
Naval Ship Research and Development Center
Washington, D.C. 20034

Code 03
Naval Air Systems Command
Washington, D.C. 20360

AIR 5301
Naval Air Systems Command
Department of the Navy
Washington, D.C. 20360

Code ORD 03
Naval Ordnance Systems Command
Washington, D.C. 20360

Code ORD 035
Naval Ordnance Systems Command
Washington, D.C. 20360

Code ORD 05413
Naval Ordnance Systems Command
Washington, D.C. 20360

Code ORD 9132
Naval Ordnance Systems Command
Washington, D.C. 20360

Oceanographer of the Navy
Washington, D.C. 20390

Commander
Naval Oceanographic Office
Washington, D.C. 20390

Chief Scientist (CNM PM-1)
Strategic Systems Project Office
Department of the Navy
Washington, D.C. 20360

Technical Division (CNM PM 11-20)
Deep Submergence Systems Project Office
Department of the Navy
Washington, D.C. 20360

Dr. A.L. Slafkosky
Scientific Advisor
Commandant of the Marine Corps (Code AX)
Washington, D.C. 20380

Librarian Station 5-2
Coast Guard Headquarters
NASSIF Building
400 7th Street, S.W.
Washington, D.C. 20591

Office of Research and Development
Maritime Administration
441 G. Street, N.W.
Washington, D.C. 20235

Division of Ship Design
Maritime Administration
441 G. Street, N.W.
Washington, D.C. 20235

National Science Foundation
Engineering Division
1800 G. Street, N.W.
Washington, D.C. 20550

Dr. G. Kulin
National Bureau of Standards
Washington, D.C. 20234

Science & Technology Division
Library of Congress
Washington, D.C. 20540

Chief of Research & Development
Office of Chief of Staff
Department of the Army
The Pentagon, Washington, D.C. 20310

Professor A. Thiruvengadam
Department of Mechanical Engineering
The Catholic University of America
Washington, D.C. 20017

Professor G. Birkhoff
Department of Mathematics
Harvard University
Cambridge, Massachusetts 02138

AIR 604
Naval Air Systems Command
Department of the Navy
Washington, D.C. 20360

Dr. A.S. Iberall, President
General Technical Services, Inc.
451 Penn Street
Yeadon, Pennsylvania 19050

Professor J.F. Kennedy, Director
Iowa Institute of Hydraulic Research
State University of Iowa
Iowa City, Iowa 52240

Professor L. Landweber
Iowa Institute of Hydraulic Research
State University of Iowa
Iowa City, Iowa 52240

Dr. Lee Segel
Department of Mathematics
Rensselaer Polytechnic Institute
Troy, New York 12180

Code 6101E
Naval Ship Engineering Center
Center Building
Prince George's Center
Hyattsville, Maryland 20782